Original Research Article

Comparative Characterization of Novel *Schizachyrium Exiles* Leaves and *Raffia Africana Otendor* For Materials Potential

ABSTRACT

The usefulness of certain indigenous plant fibers as composites in potential materials and energy applications is continuously advancing. Novel *Schizachyrium exiles* leave (SEL) and *Raffia Africana otendor* (RAOL) were characterized for their potentials using SEM, FTIR, XRD, and XRF analyses. The SEM characterization revealed the microporous and macroscopic nature of the materials that can be utilized for reinforcements in polymers, hybrids, and nano-composite fillers. In the FTIR sampling, the presence of the OH group and aliphatic C-O stretching depicted polysaccharide structure. Whereas, XRD analyses show that the crystalline nature of RAOL and SEL are capable of being used for soft structural designs. Finally, XRF revealed that some solid minerals (Ca, Si, P, K, Ti, Fe, Mg, and Al and S) exists in RAOL and SEL which can be extracted and harnessed for many materials and energy applications reminiscent of semiconductors, mesoporous materials, rechargeable batteries, solar and non-solar energy storage devices, and engineering materials.

Keywords: Composite materials, Reinforced fiber, fillers, feed resources, Plants fibers,

1. INTRODUCTION

Waste Plant resource utilization is a very important aspect of applied research for composites, hybrids, and fillers (1). The plant fiber reinforcements offer improved material composites depending on their mechanical, thermal, electrical, and rheological properties when compared to synthetic composites (2). Currently, more research work is exploring indigenous plant species that find applications in materials and energy utilization (3).

Several types of research have established the plausible potentials of *Raffia Africana otendor*, although varied species exist even within the same country. Hence, its continued characterization and documentation contribute to a better understanding as a material resource. Moreover, the plant fiber has a wide bandgap and is employed in high temperature, high power, and high-frequency materials in electronic technologies and solar energy (4). Another recent work showed that when used as epoxy hybrid composites, they offer improved automotive interior panels. Additionally, the optimum elongation is about 48.9 % and can withstand maximum stress of about 340 N/m^2 with thermal conductivity of about

0.163 WM-1K-1 (5). Hence, it finds utilization in insulating electrical materials, building designs, and even kitchen utensils (6,7).

In contrast, *Schizachyrium exile* plant potential as a material resource has a knowledge gap that needs to be investigated. It grows in open grassland with peak periods around September to November, while in some regions the peak period is during rains (8). The family is known as Lamiaceae, a wild plant herb or shrub species that belong to nine families made up of trees and grasses. It is locally known as Chen in the Gboko local government area of Benue State, Nigeria, and Himera in Sudan with characteristic termite resistant ability. Both plants are applied in craft making, thatching of huts, and local bridge construction but are threatened by chemical farming (9,10). They are utilized locally as feed resources for ruminants in Niger state, Nigeria (11). *Schizachyrium exile* is an annual plant of reddish coloration and about 10-120 cm tall having few branches from the mild culms. The leaf morphology is basal and cauline but mainly distributed in tropical Asia, tropical and temperate Africa (12,13). Therefore, for the first time to the best of our knowledge, *Schizachyrium exile* leaves are investigated and compared with *Raffia Africana otendor* for their potential energy and materials applications.

2. Material and Methods

2.1. Plant material

Raffia Africana otendor leaves (RAOL) were collected from the Adar Local Government area of Ebonyi State, Nigeria, while the *Schizachyrium exile* leaves (SEL) were collected from the Batagarawa Local Government area of Katsina State in Nigeria. The typical appearance of RAOL and SEL is shown in (figure 1) below. The RAOL and SEL leaves were washed thoroughly after collection to remove sand and dust particles. Both leaves were sun-dried (27-38^{o}C for 5 days) to brittleness and a constant weight and ground to a powder before being sieved via a 50 µm mesh. 150 g of each RAOL and SEL powder was measured and placed in a labeled tight plastic container for storage and instrumental analyses.

Figure 1: *Raffia africana otendor* plant (A) and *Schizachyrium exiles* plant (B).

2.2. Instrumental Analysis

Using the previously described standard methodology, the RAOL and SEL samples were characterized by SEM, XRD, XRF, and FTIR spectroscopy as briefly described below(14–17). The SEM process was to mount the dried samples on circular stainless-steel mold, coated with 10 nm of pure gold in a vacuum sputter and placed in the SEM sample compartment. Then SEM data of the two samples were taken using the SEM model by Phenom world Eindhoven Netherlands. During FTIR analyses, 2 g of RAOL (sample A) and 200 mg of KBr were made into a paste using a mortar. The paste was pressed together by the bolt press, cavity rotation, and hydraulic press. The sample was analyzed by FTIR spectroscopy using Perkin Elmer 8790 model instruments. The scans were performed at 400 to 4000 cm^{-1} wavelength and the procedure was repeated for SEL (sample B). XRD characterization was done by weighing out 2 g of Sample RAOL from the crucible and applying it across the XRD plate. The sample was slid into the clips sample holder and the machine door was bolted. The mini-flex software of (XRD) Equinox 300 model analyzed the sample and the process was repeated for SEL (B).

The XRF analyses were performed by weighing 1 g of Sample RAOL into XRF slim film. The film was placed inside the clip cup and tightly latched around it. The space between the cup was filled with collagen fiber and the cap was tightened. The cup was rotated to view the transparent slide and analyzed by the software X-supreme 8000 Oxford Instrument USA. The procedure was repeated for SEL (B).

3. Results and Discussion

The morphology of the *Raffia Africana otendor* leaves and *Schizachyrium exile* Leaves as investigated by SEM is revealed in Figure 2. It shows the SEM micrograph of both RAOL (LHS) and SEL (RHS) samples. From the morphological pattern, both RAOL AND SEL showed a repeating pattern that persisted throughout the entire structure. External features of particles such as contours, defects, damage, and surface layer were not seen in the SEM analysis of both samples. The SEM image of RAOL shows crystallites with small grains, while the SEL depicts crystallites with larger grain sizes. The RAOL appears to be uniformly distributed while SEL images appear in clustered sizes. In addition, the micrograph reveals the natural longitudinal elongation in RAOL. The in-growth of spherical crystallites covers the entire surface of both samples that appeared as microscopic and macroscopic pores. From the SEM analysis of the RAOL, it can be inferred that the fibers are not roundish but longitudinal in shape, which substantiates that, the fibers' can be used for continuous fiber fabrications. These longitudinal fiber/particles surface morphology plays a vital role in the case of nanocomposite materials and fillers (5,6,16).

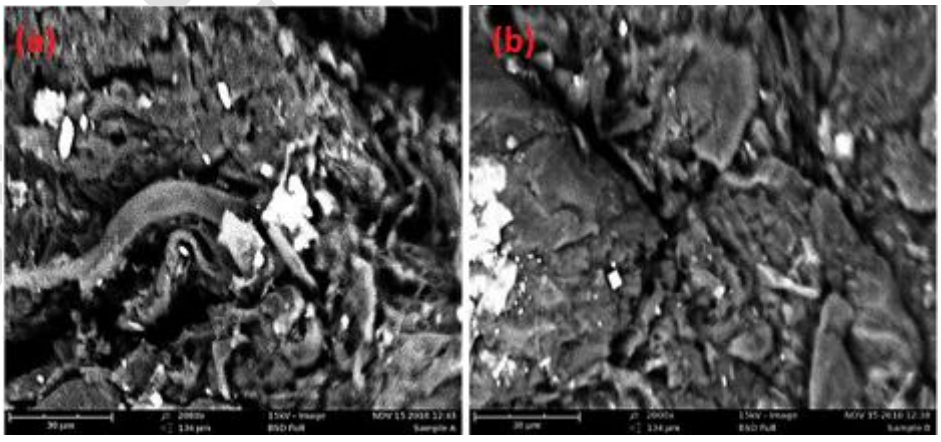

Figure 2: SEM microcragh of (a) *Raffia Africana Otendor* and (b) *Schizachyrium exiles* leaves

In *Schizachyrium exile* leave, the morphological result from SEM shows roundish rectangular-shaped particle distributions and is visible throughout the SEM analysis. It forms a similar-sized rectangular crystalline distribution with small-scattered grains. Hence, it can be used as possible fiber reinforcements in polymer composite materials. Therefore, the findings strongly suggests that the longer longitudinal fibers in RAOL will have ensuing higher density, increase in tensile strength initiated by the presence of more solid minerals (6,7).

The FTIR spectra of RAOL and SEL are shown in figure 3 and figure 4. These spectra had observable broad peaks from 3693-3283 cm^{-1} and 3280 cm^{-1} for RAOL and SEL respectively. The broad peaks at 3283 and 3280 cm^{-1} are assigned to the hydroxyl groups (-OH) stretch in RAOL and SEL. The peaks at 2918 cm^{-1} and 2918 cm^{-1} are assigned to methyl C-H asymmetry and symmetry bend respectively. At 2851-2102 cm^{-1} and 2851 - 2092 cm^{-1} are the methoxys, methyl ether O-CH_3, and C–H stretch for RAOL and SEL correspondingly. The conjugated ketone C=C and aryl-substituted C=C stretching of the carboxylic acid of carboxyl groups from hemicelluloses were seen at 1602 cm^{-1} and 1733 - 1625 cm^{-1}. The small peak at 1509 cm^{-1} and 1401 cm-1 also indicated the conjugated C–O group from aromatic ring stretch in lignin of *Raffia Africana otendor* and *Schizachyrium exile* leaves. Furthermore, the peak at 1364 - 1319 cm^{-1} refers to the C–H group de-formation in cellulose and hemicelluloses. Peaks found at 1241 and 1287 cm^{-1} were assigned to C–O stretch groups from the ether and oxyl compound group in lignin. A broad peak at 1159 - 1028 cm^{-1} is the C–C vibrations from the saturated aliphatic (alkanes) alkyl group in cellulose. The peaks in the 894 cm^{-1} range relate to the C=H out-of-plane bound vibration of lignin in RAOL.

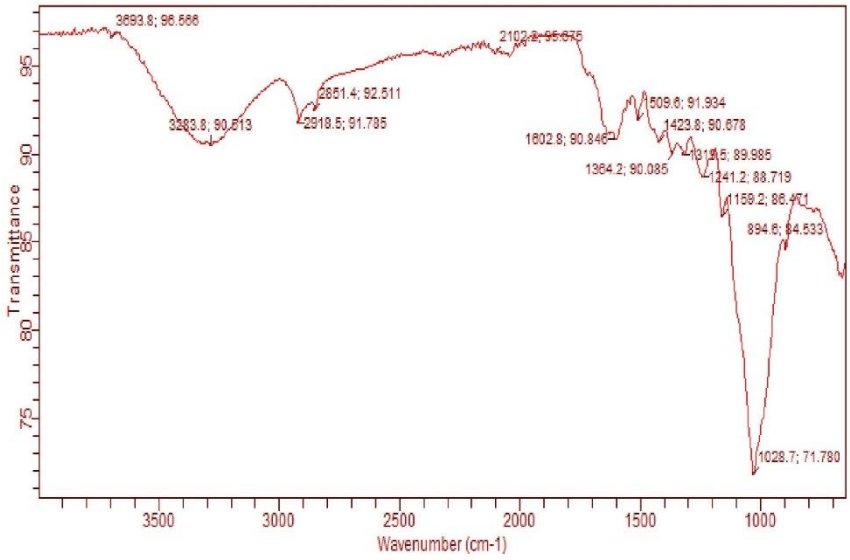

Figure 3: FTIR spectra of *Raffia Africana otendor*

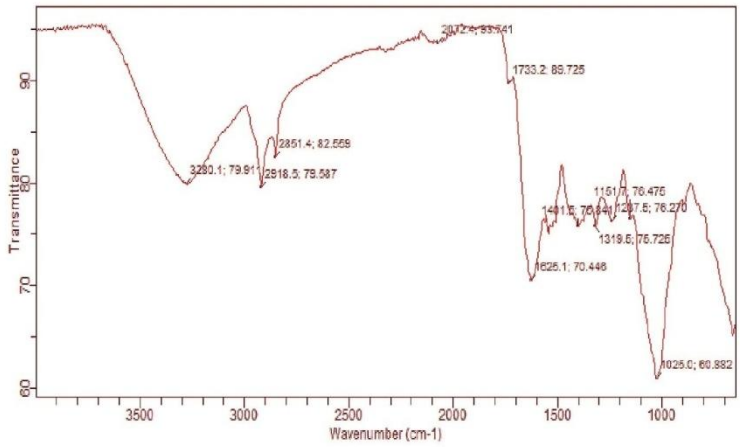

Figure 4. FTIR spectra of *Schizachyrium exile* leaves

There was the absence of stretching of the carbonyl group in SEL but present in RAOL caused by the removal of the side chain of the acetyl group of acetylated xylene during grinding. The change in absorption band amid 1625 - 1025 cm^{-1} in SEL further confirms the removal of lignin. Additionally, RAOL and SEL spectra showed changes at peaks from 1602-1159 cm^{-1} and 1625-1287 cm^{-1}, which indicated the reduction of carboxyl groups in both samples. Consequently, it was reported that the removal of amorphous parts of the fiber (lignin and hemicellulose) increases the crystallinity index of RAOL and SEL (16). Also, the presence of hydroxyl group (-OH), CH stretching of aliphatic (C-O) suggests the existence of polysaccharide structure (15). Whereas an increase in the (-OH) group depicted as peak broadening may be indicative of an increase in tensile strength (18). This result also agrees with the SEM analyses and its structural explanation. The density of RAOL is between 0.7-1.55 g/cm^3 and SEL between 0.5-1.52 g/cm^3. The values were lower than the density of some widely used synthetic fibers' such as E-glass (2.56 g/cm^3), carbon fiber (1.4-1.8

g/cm^3), and silica sand (2.4g/cm3). Hence, based on the above aforementioned functional groups, both RAOL and SEL can be used for the production of metal roofs and asphalt shingle roofs with reinforcing agents (19). In addition, the incorporation of RAOL and SEL fiber into composites will lead to the synthesis of lightweight materials with good UV resistance (20,21).

The obtained XRD patterns were presented in the 3D graph using Origin 9.0 as shown in figure 5 for clearness of important peaks. The RAOL has four prominent peaks at theta angle 10º, 15º, 25º, and 32º with high intensity.

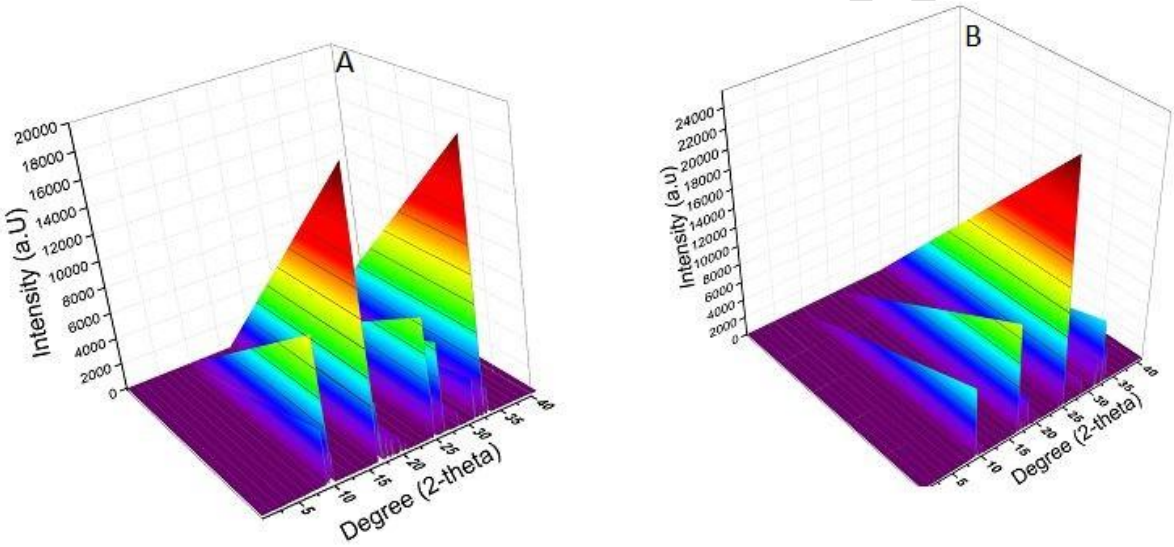

Figure 5. The XRD patterns of RAOL (A) and SEL (B)

The SEL had three less prominent peaks that shifted to 10º, 20º, and 25º theta angles. Further construal shows that the diffraction peaks appeared in patterns corresponding to phases with good crystalline nature. Higher diffraction peaks of the RAOL and SEL occur at 700 cps and 650 cps intensity, which corresponds to SiO_2 and CaO phases. The XRD pattern of *Schizachyrium exiles* leaves (sample B) showed similarity to *Raffia Africana Otendor* (sample A). However, SEL had fewer diffraction peaks of the calcium carbonate phase than silicones, as were similarly observed in FTIR. The Peak broadening depended on the crystallite size and crystallinity index of sample RAOL and SEL.

The XRD analyses further reveal that there are solid mineral elements/compounds in higher amounts in RAOL than in SEL due to extra superior diffraction angles. Additionally, the presence of theta at 15/16º and 25º reveals the crystalline nature of the samples. This remarkably is a pointer to potential soft structural design applications due to an increase in tensile strength as recognized in FTIR spectrum and SEM analyses (4,18,21).

The results obtained from the XRF study are expressed in figure 6 below in weight percent. The percent values plotted to show that sodium is negligible in both RAOL and SEL. This shows that Na_2O is not an essential compound in the growth and development of SEL and RAOL. Similarly, Cr_2O_3 and TiO_2 were lowest in SEL while Cr_2O_3 and ZnO were lowest in RAOL. The value of Magnesium content in RAOL at 1.27 is seven times smaller than SEL at

9.70 wt. %. This shows that magnesium is very important in the cellular function of RAOL. The concentrations of Al_2O_3, Cl, and K_2O in both Samples did not differ significantly. The outcome obtained for silicon concentration in RAOL (Sample A) was obvious at 53 Wt. % than SEL (Sample B) at 19.8 Wt. %. Also, silicon was present in larger amounts, which suggests that the material can be applied in the development of semiconductors. Hence, it does not absorb heat but rather reflects it to the environment. The silicon when extracted has potential for silicon solar cells in industrial construction with clay, silica sand, and stone as composites. It is already applied in Portland cement for mortar as well as suitable for local and traditional roofing material (1,9,22).

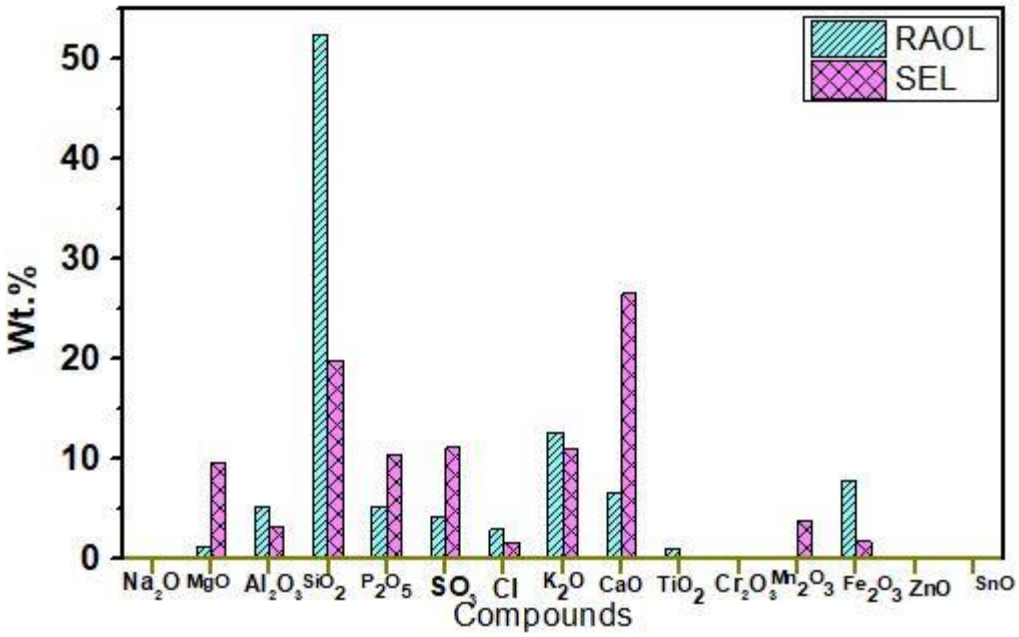

Figure 6. XRF elemental analyses of RAOL and SEL

Phosphorus content for SEL is twice that of RAOL. Phosphorus is a component of nucleic acid and photosynthesis, involved in energy transfer. The plant possibly utilizes added phosphorous for frequent flowering and budding that eventually leads to pollination. Thus, SEL can be harnessed for phosphorus-based mesoporous materials for energy conversion and storage (23). The concentration of sulfur content in RAOL and SEL were 4.34 and 11.19 and can be processed for the development of lead-acid batteries, glass, and explosives. Moreover, there is a recent sulfur-based technology for storing solar energy (24,25). Potassium Wt. % was more than 10% in both samples. The potassium element is a major inorganic cation that regulates osmotic potential. Hence, it is needed for plant growth. The element can be employed in the development of potassium-ion rechargeable batteries with the potential to lower-cost alternatives to conventional batteries (26–28).

The result shows that the concentration of calcium in RAOL and SEL were 6.66 and 26.6 respectively. Calcium is responsible for the synthesis of cell wall membrane function in plants; hence, it protects SEL from heat stresses by improving stomata functions. The calcium element can be extracted for the development of thermo-chemical energy storage devices based on CaO composite materials (29). Manganese content was insignificant in

RAOL but small in SEL. It presents the possibility for manganese-hydrogen-based batteries for grid-scale and energy storage (30).

Titanium is very low in both samples. It is paramagnetic and has low electrical and thermal conductivity coupled with photocatalytic ability. Iron is higher in RAOL than SEL and may suggest that RAOL provides improved reinforcement than SEL in composite materials and infrastructure development (31). Zinc is required to support chlorophyll biosynthesis. The tin metal amount is negligible and considered a non-essential element in RAOL and SEL. Jointly, TiO2, ZnO, and ZnO are used as mesoscopic semiconductors (32). Magnesium in appreciable quantity (SEL) can be used for magnesium hydride-based materials and compounds for hydrogen and energy storage (33). While aluminum can provide energy efficiency improvement, product design, and reduced material waste when utilized in heat exchange, motor components, truck chassis parts, and glazing systems (34)

CONCLUSION

The relative characterization of *Raffia Africana Otendor* and *Schizachyrium exiles* leaves was achieved using SEM, XRD, FTIR, and XRF spectroscopy. Findings showed that RAOL exists in longitudinal arrangements while SEL exists in spherical arrangements. As a consequence of their inherent crystallite sizes, both samples had the presence of C-H stretching and OH group which improves tensile strength giving them a potential advantage as composites, fillers, and reinforcements. However, a relative study showed that several challenges like inferior mechanical properties, higher water absorption, energy absorption, and visco-elastic properties still affect their performance as polymer composites and nanofillers. Nevertheless, fiber treatment is one of many solutions suggested to improve composite properties (35). Consequently, it is recommended that a comprehensive novel mechanical characterization of *Schizachyrium exiles* leaves as a composite material is carried out to understand the mechanical and materials behavior. It is therefore projected that these plant fibers may gradually progress to support conventional reinforcements and fillers in material composites.

References

1. Saba N, Tahir M, Jawaid M. Review on potentiality of nano filler/natural fiber filled polymer hybrid composites. Polymer (Guildf). 2014;6:2247–73.
2. Mahmud S, Hasan KMF, Jahid MA, Mohiuddin K, Zhang R, Zhu J. Comprehensive review on plant fiber-reinforced polymeric biocomposites. J Mater Sci. 2021;56(12):7231–64. Available from: https://doi.org/10.1007/s10853-021-05774-9
3. Dixit S, Goel R, Dubey A, Shivhare PR, Bhalavi T. Natural Fibre Reinforced Polymer Composite Materials - A Review. Polym from Renew Resour. 2017;1;8(2):71–8. Available from: https://doi.org/10.1177/204124791700800203
4. Ufere E, Okpala O. Synthesis and Characterization of undoped raffia palm and oil bean doped lead chloride (PbCl2) crystal in silica Gel. Int J Sci Eng Res. 2016;7(1):583–92.
5. Nyior G., Aye S., Tile S. Study of Mechanical Properties of Raffia Palm Fibre/Groundnut Shell Reinforced Epoxy Hybrid Composites. J Miner Mater Charact Eng. 2018;6:179–92.
6. James R, Tamunoiyowuna S. Investigation of Thermal Conductivity of Raphia Fibre (Piassava) from Raphia Hookeri. Int J Appl Sci Math Theory. 2016;2(2):11–7.
7. Odera R, Onukwuli O, Osoka E. Stress and Strain Characteristics of Raffia Palm

Fibre under Varying Conditions. Int J Chem Eng Res. 2011;3(2):159–66.
8. Mitra S, Soban K. Biodiversity impact and assessment: Diversity of grass flora of West Bengal with special reference to their utility. 2nd ed. Jaipur: India: Pointer Publishers.; 2011. 23–109 p.
9. Shomkegh S, Mbakwe F, Sale F. Ethno botanical Survey of Wild Plants Utilized for Craft Making and Local Construction among the Tiv People of Benue State, Nigeria. J Agric Ecol Res Int. 2016;9(3):1–11.
10. Sulieman HM, Buchroithner MF, Elhag MM. Use of local knowledge for assessing vegetation changes in the Southern Gadarif Region, Sudan. Afr J Ecol. 2012 1;50(2):233–42. Available from: https://doi.org/10.1111/j.1365-2028.2011.01318.x
11. Nourou A, Nasreldin B, Abdoulaye S, Ignatius V. Effect of urea treatment of roughages and in vitro ingestibility of available feed resources in Maradi area of Niger. Am J Agric For. 2018;6(4):78–83.
12. Ibrahim author. K (Kamal M. Grasses of Mali. Washington, D.C. : Smithsonian Institution Scholarly Press,;
13. Arthan W, McKain MR, Traiperm P, Welker CAD, Teisher JK, Kellogg EA. Phylogenomics of Andropogoneae (Panicoideae: Poaceae) of Mainland Southeast Asia. Syst Bot. 2017:1;42(3):418–31. Available from: https://doi.org/10.1600/036364417X696023
14. Elenga R., Djemia P, Tingaud D, Chauveau T, Maniongui J., Dirras G. Effects of alkali treatment on the microstructure, composition, and properties of the Raffia textilis fiber. Bioresources. 2013;8(2):2934–49.
15. Majekodunmi U. Characterization of Raphia Hookeri gum for the purpose of being used as a pharmaceutical excipient. World J Pharm Res. 2016;5(2):86–97.
16. Odera R, Onukwuli O, Atunanya C. Characterization of the thermo-microstructural analysis of raffia palm fibers proposed for roofing sheet production. J Miner Matererials Charact Eng. 2015;3:335–43.
17. Ahmed A, Abdullah M, Wood K, Hamza M, Othman R. Determination of some trace elements in marine sediment using ICP-MS and XRF (A Comparative Study). Orient J Chem. 2016;29(3):645–53.
18. Fadele O, Oguocha INA, Odeshi A, Soleimani M, Karunakaran C. Characterization of raffia palm fiber for use in polymer composites. J Wood Sci. 2018;64(5):650–63. Available from: https://doi.org/10.1007/s10086-018-1748-2
19. Foster B. Establishment, Competition and the Distribution of Native Grasses among Michigan Old-Fields. J Ecol. 1999;87(3):467–89.
20. Danewalia SS, Sharma G, Thakur S, Singh K. Agricultural wastes as a resource of raw materials for developing low-dielectric glass-ceramics. Sci Rep. 2016;6(1):24617. Available from: https://doi.org/10.1038/srep24617
21. Eze-Uzomaka O, O. Nwadiuto O. Appraisal of coir fiber- cement mortar composite for low cost roofing purposes. African J Sci Technol. 2009;8(1):6–15.
22. Mohammed L, Ansari M, Pua G, Jawaid M, Islam S. A review on natural fiber reinforced polymer composite and its applications. Int J Polym Sci ence. 2015;Article ID:1–15.
23. Mei P, Kim J, Kumar NA, Pramanik M, Kobayashi N, Sugahara Y, et al. Phosphorus-Based Mesoporous Materials for Energy Storage and Conversion. Joule. 2018;2(11):2289–306. Available from: https://www.sciencedirect.com/science/article/pii/S2542435118303477
24. Seyfaee A, Jafarian M, Moumin G, Thomey D, Corgnale C, Sattler C, et al. Integration assessment of the hybrid sulphur cycle with a copper production plant. Energy Convers Manag. 2021;249:114832. Available from: https://www.sciencedirect.com/science/article/pii/S0196890421010086
25. Liu C, He Z, Li Y, Liu A, Cai R, Gao L, et al. Sulfur contributes to stable and efficient carbon-based perovskite solar cells. J Colloid Interface Sci. 2022;605:54–9. Available

from: https://www.sciencedirect.com/science/article/pii/S0021979721011255
26. Hwang J-Y, Myung S-T, Sun Y-K. Recent Progress in Rechargeable Potassium Batteries. Adv Funct Mater. 2018 Oct 1;28(43):1802938. Available from: https://doi.org/10.1002/adfm.201802938
27. Xu Y-S, Duan S-Y, Sun Y-G, Bin D-S, Tao X-S, Zhang D, et al. Recent developments in electrode materials for potassium-ion batteries. J Mater Chem A. 2019;7(9):4334–52. Available from: http://dx.doi.org/10.1039/C8TA10953B
28. Wang H, Wang Y, Wu Q, Zhu G. Recent developments in electrode materials for dual-ion batteries: Potential alternatives to conventional batteries. Mater Today. 2021; Available from: https://www.sciencedirect.com/science/article/pii/S1369702121003953
29. Yuan Y, Li Y, Zhao J. Development on Thermochemical Energy Storage Based on CaO-Based Materials: A Review. Vol. 10, Sustainability . 2018.
30. Chen W, Li G, Pei A, Li Y, Liao L, Wang H, et al. A manganese–hydrogen battery with potential for grid-scale energy storage. Nat Energy. 2018;3(5):428–35. Available from: https://doi.org/10.1038/s41560-018-0147-7
31. Razzaq A, Ajaz T, Li JC, Irfan M, Suksatan W. Investigating the asymmetric linkages between infrastructure development, green innovation, and consumption-based material footprint: Novel empirical estimations from highly resource-consuming economies. Resour Policy. 2021;74:102302. Available from: https://www.sciencedirect.com/science/article/pii/S0301420721003123
32. Hoye RLZ, Musselman KP, MacManus-Driscoll JL. Research Update: Doping ZnO and TiO2 for solar cells. APL Mater. 2013; 1;1(6):60701. Available from: https://doi.org/10.1063/1.4833475
33. Yartys VA, Lototskyy M V, Akiba E, Albert R, Antonov VE, Ares JR, et al. Magnesium based materials for hydrogen based energy storage: Past, present and future. Int J Hydrogen Energy. 2019;44(15):7809–59. Available from: https://www.sciencedirect.com/science/article/pii/S0360319919300072
34. Haraldsson J, Johansson MT. Energy Efficiency in the Supply Chains of the Aluminium Industry: The Cases of Five Products Made in Sweden. Vol. 12, Energies . 2019.
35. Fadele O, Oguocha INA, Odeshi AG, Soleimani M, Tabil LG. Effect of chemical treatments on properties of raffia palm (Raphia farinifera) fibers. Cellulose. 2019;26(18):9463–82. Available from: https://doi.org/10.1007/s10570-019-02764-8